Electrical transport studies of the $La_{2-x}Sr_xCuO_4$ system near the metal-insulator-semiconductor transition and the effect of Zn doping on localization

Electrical transport studies of the $La_{2-x}Sr_xCuO_4$ system near the metal–insulator–semiconductor transition and the effect of Zn doping on localization

V P S Awana†, S K Agarwal†, M P Das‡ and A V Narlikar†

† National Physical Laboratory, Dr K S Krishnan Road, New Delhi 110012, India
‡ Research School of Physical Sciences, The Australian National University, Canberra, ACT 2601, Australia

Abstract. Electrical transport properties of $La_{2-x}Sr_xCuO_4$ up to $x = 0.4$ have been systematically investigated. A gradual change taking place in the sequences semiconducting–non-superconducting, semiconducting–superconducting, metallic–superconducting and metallic–non-superconducting has been observed. The results provide the experimental evidence for a transition from metallic behaviour at high temperatures to a variable-range hopping (VRH) regime at low temperatures. A crossover from 3D VRH to 2D VRH has been observed when the system changes from a semiconducting–non-superconducting to a semiconducting–superconducting type. The samples with different Sr concentrations were further doped with zinc at the Cu site, and the resulting effect on superconductivity and normal-state resistivity has been examined. The two competing processes, namely the increase in the hole concentration with Sr addition and the localization of charge carriers due to Zn substitution have been discussed.

1. Introduction

It is now well established that an optimum carrier concentration is essential for attaining high-temperature superconductivity [1]. The carrier concentration may be changed by varying the oxygen content in the $YBa_2Cu_3O_{7-y}$ compound [2] or by the partial replacement of La^{3+} ions by Sr^{2+} ions in the $La_{2-x}Sr_xCuO_4$ compound [3]. From this point of view, while $YBa_2Cu_3O_{7-y}$ has been extensively studied over a wide range of y-values [2, 4], most of the reported work on the $La_{2-x}Sr_xCuO_4$ system [5, 6] has been confined to near the optimum carrier density corresponding to the Sr concentration of $0.10 \leqslant x \leqslant 0.20$. Moreover, the effects arising from various cationic substitutions in this system have been studied primarily to examine the normal-state electronic transport behaviour [7] and relatively less attention has been paid to the ensuing effects when the carrier concentration deviates on either side of the optimum concentration.

In this paper we report systematic transport measurements on $La_{2-x}Sr_xCuO_4$ with $0 \leqslant x \leqslant 0.40$. The wide range of compositions with close intervals of about $x = 0.02$ allows one to explore carrier concentrations both lower and higher than the optimum carrier concentration found for the $La_{2-x}Sr_xCuO_4$ system. The chemical iodometric technique has been used to estimate the oxygen content and the effective

Cu valence in the samples, which determines the number of holes in the system. Transport measurements provide the experimental evidence for a transition from the metallic behaviour at high temperatures to the variable-range hopping (VRH) regime at low temperatures [8]. Such a transition is seemingly controlled by the effective Cu valence which in turn is determined by the Sr content. A dimensionality change from 3D to 2D VRH has been observed with increasing Sr concentration. Samples with varying Sr content have been further doped with zinc at the Cu site. Such a study is expected to throw considerable light on the interrelation between the presence of Sr and Zn in the system and the T_c behaviour as well as on further localization effects of charge carriers due to zinc doping.

2. Experimental details

Various samples in the $La_{2-x}Sr_xCuO_4$ system $(0 \leqslant x \leqslant 0.40)$ were synthesized by the solid state reaction of appropriate quantities of well mixed metal oxides and carbonates of greater than 99.99% purity. The calcination was carried out at 940, 950 and 960 °C each for 15 h, followed by quenching to ambient temperature with intermediate grindings in between. The reacted materials, pulverized and cold pressed into rectangular slabs suitable for resistivity measurements, were oxygen annealed at 975 °C for 15 h and then furnace cooled to room temperature over a span of about 8 h. A similar synthesis procedure was adopted for the series $La_{2-x}Sr_xCu_{1-x'}Zn_{x'}O_4$ for $0.15 \leqslant x \leqslant 0.40$ and different x' between 0 and 0.16. XRD patterns were recorded using Cu $K\alpha$ radiation at room temperature to check primarily the homogeneity of the samples. Four-probe resistivity data of the samples were acquired in the temperature range 4.2–300 K using a liquid-helium cryostat with a carbon glass resistor temperature sensor in conjunction with a Lakeshore cryogenic thermometer. The entire measurement system consisting of the nanovoltmeter, constant-current source and temperature controller and indicator was hooked up to a HP216 system controller for automatic data acquisition and control. The effective Cu valence was determined by the conventional iodometric titration technique [9, 10]. The oxygen content was then calculated taking La to be in the 3+ and Sr to be in the 2+ valence state.

3. Results and discussion

Figure 1 shows resistivity ρ versus temperature plots for the $La_{2-x}Sr_xCuO_4$ system with $0 \leqslant x \leqslant 0.40$. The inset shows ρ versus T plots for $0 \leqslant x \leqslant 0.08$. The undoped sample with $x = 0$, i.e. La_2CuO_4, behaves like an insulator with a high resistivity of 530 mΩ cm at 250 K. As x increases, metallic behaviour is observed at higher temperatures with a semiconducting-like regime at lower temperatures. The crossover temperature (indicated by vertical arrows) decreases with increasing x. No such turning point is observed for $x = 0.15$ which corresponds to the optimum T_c of 36 K [11]. No superconducting transition is observed for $0 \leqslant x \leqslant 0.06$ while, for $0.08 \leqslant x \leqslant 0.27$, superconductivity is observed. Again, for $0.27 \leqslant x \leqslant 0.40$, the superconductivity transition is not revealed; only the metallicity is seen to increase with increasing x (figure 2). The normal-state resistivity ρ_n (measured at 250 K) decreases with increasing x. Such a behaviour is depicted in the inset of figure 2. The semiconducting-like behaviour of the resistivity exhibited in the concentration
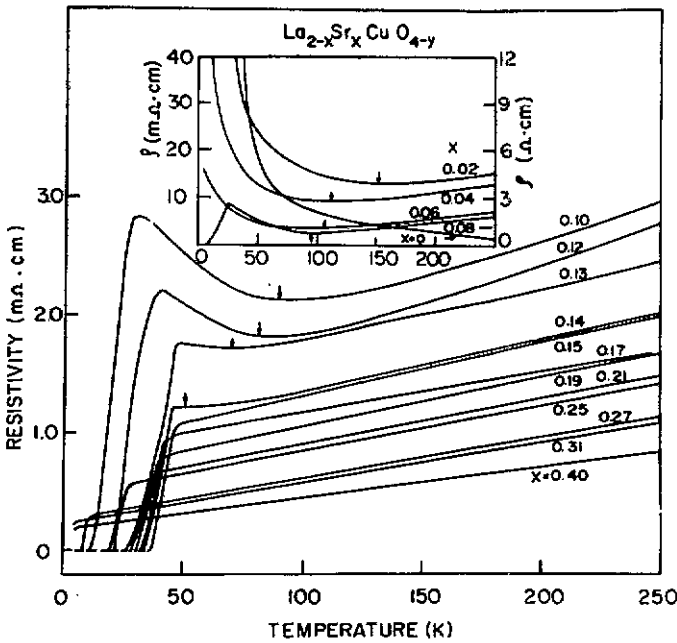
Figure 1. ρ versus T behaviour of the $La_{2-x}Sr_xCuO_4$ system for $0 < x < 0.40$. The resistivity of the $x = 0.08$ sample has been multiplied by 3.

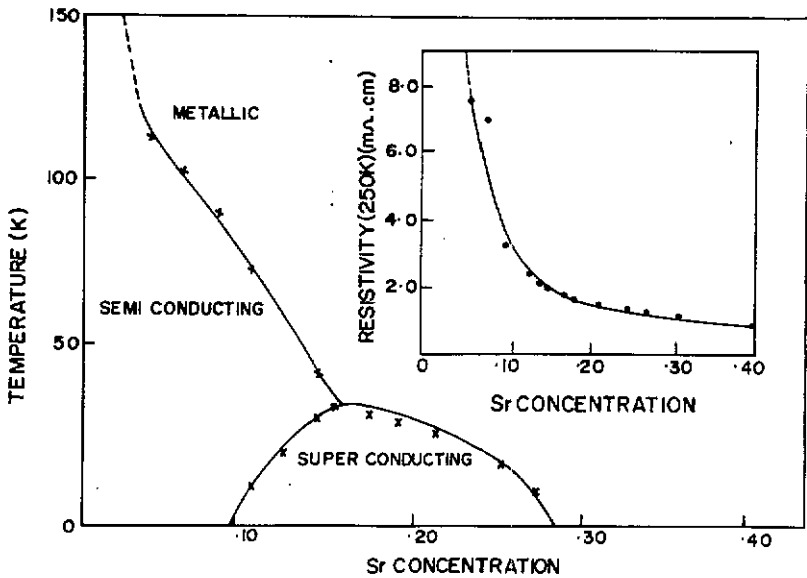**Figure 2.** Phase diagram followed by the $La_{2-x}Sr_xCuO_4$ system. The inset shows the ρ_n (250 K) versus x behaviour.

range $0 \leqslant x \leqslant 0.12$ in the low-temperature regime can be fitted to the general VRH equation

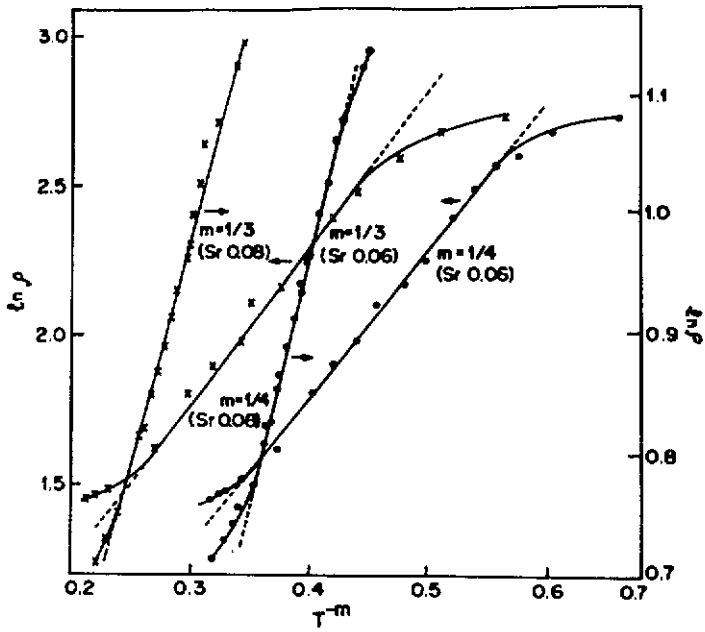$$\rho(T) = \rho_0 \exp[(T_0/T)^m] \tag{1}$$

Figure 3. ln ρ versus T^{-m} plots for $x = 0.06$ and 0.08 samples for both $m = \frac{1}{3}$ and $m = \frac{1}{4}$ values.
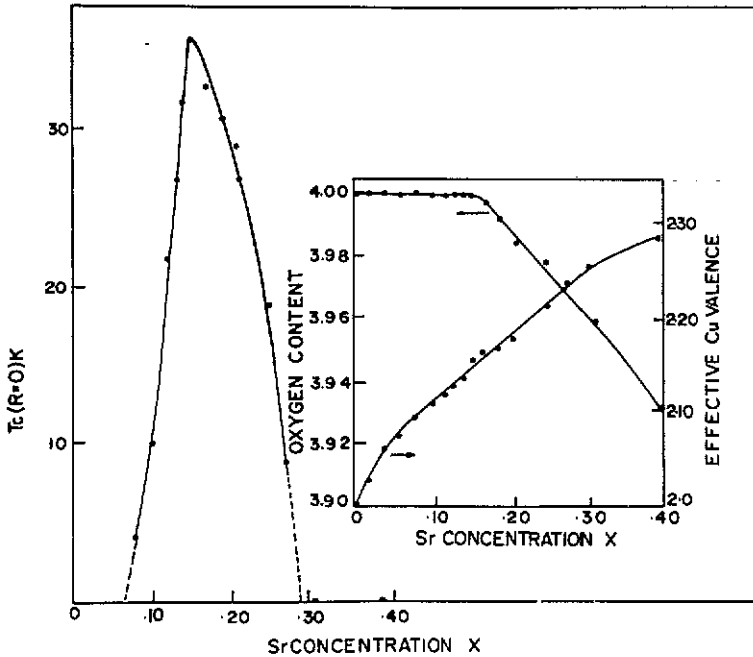

Figure 4. $T_c(R = 0)$ variation with x for the $La_{2-x}Sr_xCuO_4$ system. The inset shows the oxygen content and effective Cu valence as a function of x.

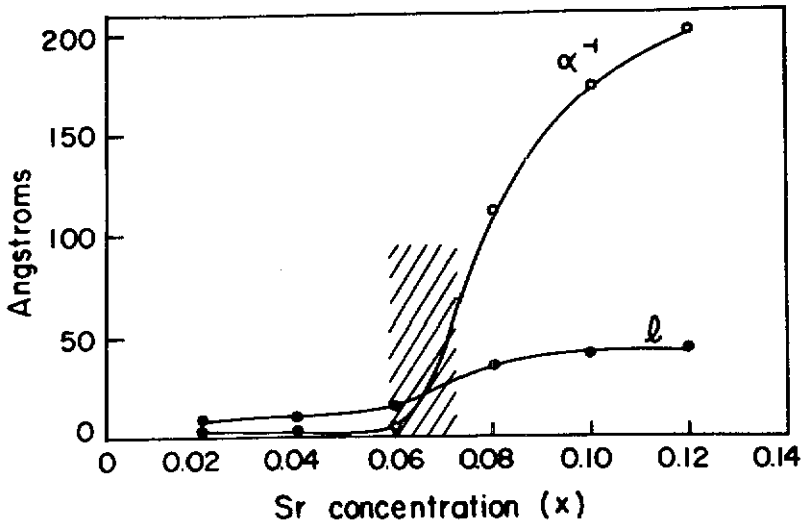**Figure 5.** Localization length, α^{-1}, and electron mean free path, l, variation with x.
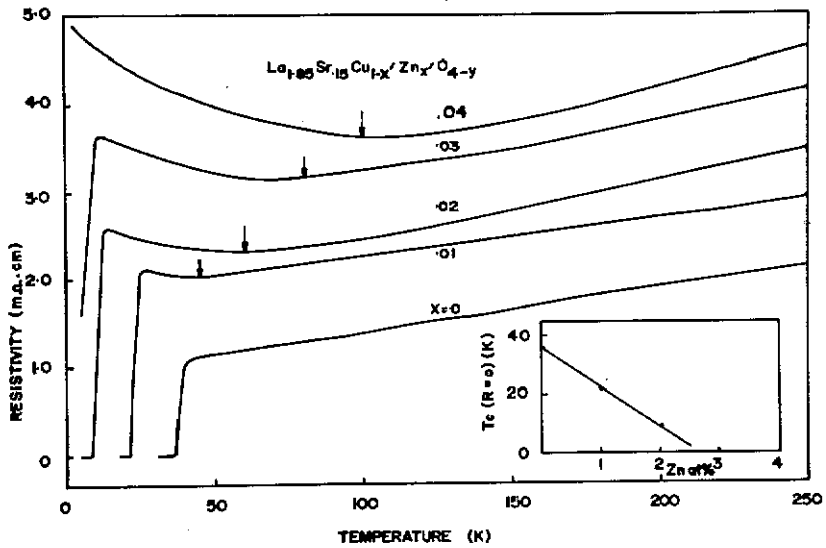

Figure 6. ρ versus T behaviour of the La$_{1.85}$Sr$_{0.15}$Cu$_{1-x'}$Zn$_{x'}$O$_4$ system for $0 < x' < 0.04$. The inset shows the behaviour of $T_c(R = 0)$ with Zn concentration.

where the exponent m distinguishes between the 2D ($m = \frac{1}{3}$) and 3D ($m = \frac{1}{4}$) VRH processes [12, 13]. The VRH has been reported in the various high-T_c cuprates. Ellman *et al* [8] observed for La$_{2-x}$Sr$_x$CuO$_4$ in the low-temperature (below 8 K) region an exponent $m = \frac{1}{2}$ for $x = 0.02$ and $m = \frac{1}{4}$ for the $x = 0.05$ sample [8]. The EuBa$_2$Cu$_3$O$_{7-y}$ system was seen to have $m = \frac{1}{3}$ (2D VRH) in the temperature range 14–125 K [14]. In the case of Bi$_2$Sr$_2$Ca$_{1-x}$Y$_x$Cu$_2$O$_8$ a variation in the exponent has been reported by different workers; for example Tamegai *et al* [15] reported $m = \frac{1}{3}$ while Yoshizaki *et al* [16] reported $m = \frac{1}{4}$. Mandal *et al* [17] observed for the same system 2D VRH for $x > 0.55$ while at $x = 0.55$ it was difficult to ascertain
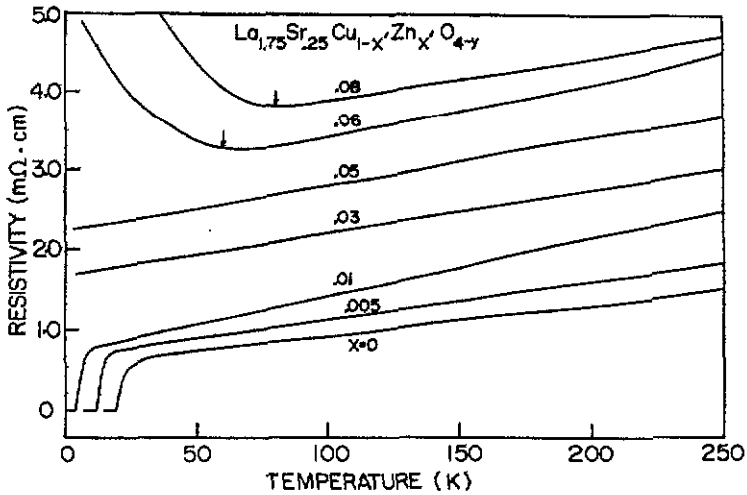
Figure 7. ρ versus T behaviour of the $La_{1.75}Sr_{0.25}Cu_{1-x'}Zn_{x'}O_4$ system for $0 < x' < 0.08$.
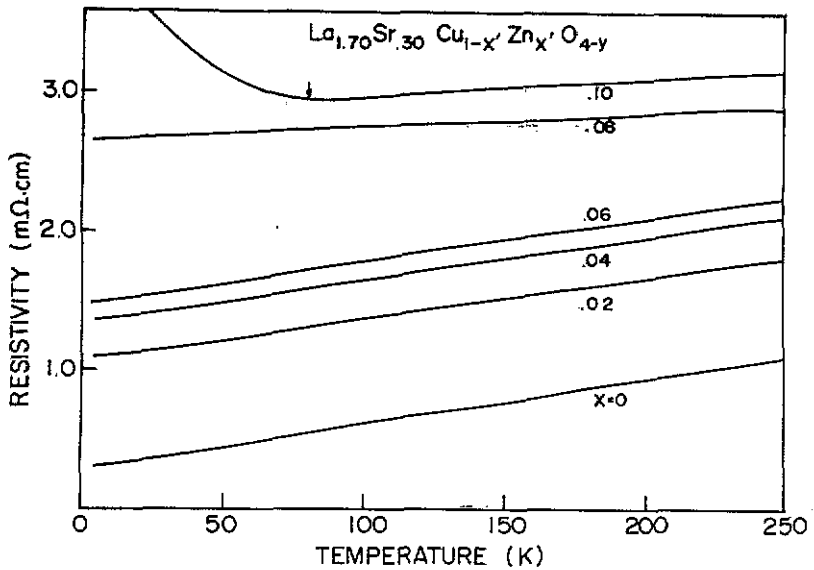
Figure 8. ρ versus T behaviour of the $La_{1.70}Sr_{0.30}Cu_{1-x'}Zn_{x'}O_4$ system for $0 < x' < 0.10$.

the exponent value of $\frac{1}{3}$ or $\frac{1}{4}$ as the system was undergoing a dimensionality crossover. For the data reported here a value of the exponent m close to $\frac{1}{4}$ has been found in the range $0 \leqslant x \leqslant 0.06$, while for $0.08 \leqslant x \leqslant 0.12$ it comes out as close to $\frac{1}{3}$, indicating 3D and 2D VRH processes to be operative in these ranges. Typical curve fittings of $\ln \rho$ versus T^{-m} based on equation (1) for $x = 0.06$ and $x = 0.08$ samples with both $m = \frac{1}{3}$ and $m = \frac{1}{4}$ values are shown in figure 3, indicating the subtle difference between these fittings. The exponents $m = \frac{1}{4}$ and $m = \frac{1}{3}$ have been found for $x = 0.06$ and 0.08 samples, respectively, showing a higher-temperature-range fitting compared with the other values of exponents. Interestingly, superconductivity is
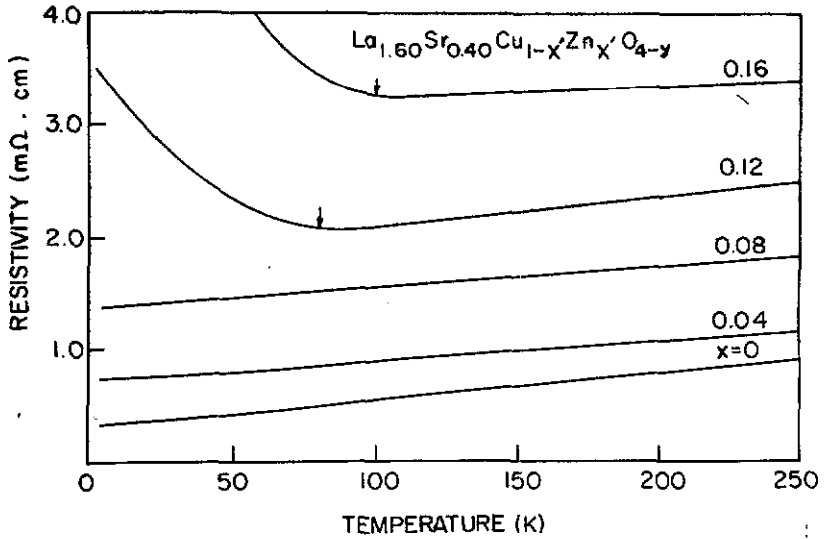
Figure 9. ρ versus T behaviour of the La$_{1.60}$Sr$_{0.40}$Cu$_{1-x'}$Zn$_{x'}$O$_4$ system for $0 < x' < 0.16$.

observed for $0.08 \leqslant x \leqslant 0.12$ (2D VRH regime) while no superconductivity is found in the range $0 \leqslant x \leqslant 0.06$, which corresponds to the 3D VRH regime. The behaviour of the change from 3D to 2D VRH observed by us as a function of Sr concentration seems to be in good accord with the recent report [18] on Gd-substituted at the Ca site in Bi-2:1:2:2 superconductor. The effective Cu valence which changes with Sr concentration (inset of figure 4) seems to be the controlling factor for such a crossover. Table 1 lists the various parameters such as ρ_n, the crossover temperature, T_c, the oxygen content and the effective Cu valence for the different samples. Accordingly the 3D VRH process seems to be operative for the samples having an effective Cu valence between 2.0 and 2.07 while, for effective Cu valences between 2.07 and 2.11, the 2D VRH process is indicated. Such a crossover of the dimensionality with Sr content (and thereby the effective Cu valence) and the associated superconductivity in conjunction with 2D VRH qualitatively agrees with a theoretical model [19] that examines the competition between superconductivity and localization. The localization length α^{-1} is defined by the approximate VRH relation [12, 20] as $\alpha^{-1} = [k_B T_0 N(E_F)/16]^{-1/3}$ (for the 3D case) and $\alpha^{-1} = [4\pi k_B T_0 N(E_F)/27]^{-1/2}$ (for the 2D case). It increases with increasing Sr concentration as a result of changes in T_0 and $N(E_F)$. It is worth pointing out that α^{-1} decreases in the Bi-2:1:2:2 compound with increasing Y at Ca sites. Here the carrier density (and hence the metallicity) decreases with increasing Y content unlike in the present case where Sr introduces more holes into the system, thereby increasing the metallicity. The density $N(E_F)$ of states varies in the range 2–13 states eV^{-1} cell as x increases [21]. The localization length of the system in the VRH regime can be compared with the electronic mean free path [22] $l = 4\pi v_F/\omega_p^2 \rho(x)$, where v_F is the Fermi velocity and $\omega_p = (4\pi n e^2/m^*)^{1/2}$ is the plasma frequency (m^* and n are the effective carrier mass and concentration, respectively). Figure 5 shows the localization length and mean free path variation with Sr concentration for $0 \leqslant x \leqslant 0.12$ taking $v_F = 0.95 \times 10^7$ cm s^{-1} and $\hbar\omega_p(x=0) = 0.63$ eV [20]. Initially both α^{-1} and l increase slowly with increasing

x up to 0.06. α^{-1} increases sharply in the region of $x = 0.06$–0.08 where the system is undergoing the insulator-to-metal transition and diverges as T_0 approaches zero, i.e. at the superconducting transition point. The two curves intersect each other near $x = 0.07$ which significantly is the experimentally observed range for the VRH regime crossover from 3D to 2D in the system. Accordingly, for $l < \alpha^{-1}$, the system corresponds to 2D VRH and the superconducting transition is observed while, for $\alpha^{-1} < l$, 3D VRH is observed with no superconductivity.

Table 1. Quantitative data for the $La_{2-x}Sr_xCuO_{4-y}$ system ($0 \leqslant x \leqslant 0.4$).

Sr content x	$\rho_n(250\ K)$ (mΩ cm)	$T_c(R = 0)$ (K)	Crossover temperature (K)	Oxygen content	Effective Cu valence
0.00	530.00	—	—	4.00	2.00
0.02	15.00	—	150	4.01	2.03
0.04	12.50	—	116	4.00	2.06
0.06	7.50	—	105	4.00	2.07
0.08	3.00	4.2	95	4.00	2.09
0.10	2.90	10.2	90	4.01	2.10
0.12	2.78	22.0	80	4.00	2.11
0.13	2.45	27.0	70	4.00	2.12
0.14	2.10	32.0	50	4.00	2.13
0.15	2.00	36.0	—	4.00	2.15
0.17	1.67	33.0	—	3.99	2.16
0.19	1.63	31.0	—	3.99	2.17
0.21	1.50	27.0	—	3.98	2.19
0.25	1.41	19.0	—	3.98	2.21
0.27	1.13	9.0	—	3.97	2.23
0.31	1.10	—	—	3.96	2.24
0.40	0.81	—	—	3.93	2.27

Of the different substitutions (at the Cu site) in the various high-T_c cuprates, Zn at the Cu site has been seen to have a drastic effect on T_c and on the normal-state behaviour [23, 25]. Recent reports [23] have indicated the occupation of divalent Zn in the Cu–O planar structure. T_c depression and normal-state properties have been found to be associated with carrier localization effects [26]. To explore this aspect, different amounts of Zn doping in the $La_{2-x}Sr_xCuO_{4-y}$ system have been attempted. Figure 6 shows the ρ versus T plots for the $La_{1.85}Sr_{0.15}Cu_{1-x'}Zn_{x'}O_{4-y}$ system with $0 < x' < 0.04$. The inset shows the $T_c(R = 0)$ behaviour with Zn doping. The crossover temperature from metallic to semiconductor behaviour is seen to increase with increase in Zn content. The ρ versus T curves in the semiconducting regime could not be fitted well to equation (1), indicating that, while localization may be there in the system, clear evidence for the VRH process is seemingly lacking. The drastic rate of T_c depression (13 K (at.%)$^{-1}$) by the Zn doping (inset) has been seen for other high-T_c cuprates also [24]. The normal-state resistivity increases with increasing Zn concentration and has been discussed in detail elsewhere [23]. Figure 7 shows the ρ versus T plots for the $La_{1.75}Sr_{0.25}Cu_{1-x'}Zn_{x'}O_{4-y}$ system with $0 \leqslant x \leqslant 0.08$. For $x' = 0$ the sample possesses a T_c of 19 K which decreases with increasing Zn content. The T_c depression rate is similar (about 13 K (at.%)$^{-1}$) to that for the $x = 0.15$ sample. $\rho_n(250\ K)$ again increases with increasing Zn in the system. For $x' = 0.05$, the resistivity behaviour is metallic down to 4.2 K while, for $x' = 0.06$ and 0.08, the semiconducting-like behaviour occurs at low

temperatures. For a Sr content of 0.25 which leads to more holes, more Zn is needed to produce localization at lower temperatures. In the low-temperature range where semiconducting behaviour occurs for the $x = 0.06$ and 0.08 samples, fitting with equation (1) yielded a value of m close to $\frac{1}{3}$. Figure 8 shows the ρ versus T plots for the La$_{1.70}$Sr$_{0.30}$Cu$_{1-x'}$Zn$_{x'}$O$_{4-y}$ system with $0 < x' < 0.10$. A pure sample with $x' = 0$ does not show any T_c but the resistivity behaviour is completely metallic down to 4.2 K. ρ_n, however, increases with increasing Zn content. Up to 8 at.% Zn in the system a metallic behaviour is observed down to 4.2 K, while the sample with 10 at.% Zn becomes semiconducting-like at low temperatures. It is interesting to note that, for a Sr content of 0.30, to produce localization more Zn is needed than in the $x = 0.25$ samples. This is attributed to there being more holes in the $x = 0.30$ sample than in the $x = 0.15$ and 0.25 samples. This contention is further strengthened by the results on La$_{1.60}$Sr$_{0.40}$Cu$_{1-x'}$Zn$_{x'}$O$_{4-y}$ system (figure 9). Here the curve fitting to equation (1) in the semiconducting region also shows a 2D VRH behaviour. All these results indicate that an intrinsic competition is taking place between the increase in the hole concentration, resulting from the increase in Sr doping, and the enhanced localization produced by the increase in Zn substitution.

Acknowledgments

References

[1] Torrance J B, Tokura Y, Nazzal N I, Bezing A, Huang T C and Perkin S S P 1988 *Phys. Rev. Lett.* **61** 1127
[2] Cava R J, Batlogg B, Chen C H, Rietman E A, Zahurak S M and Werder D 1987 *Nature* **329** 429; *Phys. Rev.* B **36** 5719
[3] Shafer M W, Penny T and Olson B L 1987 *Phys. Rev.* B **36** 4047
[4] Jorgenson J D, Beno M A, Hinks D G, Soderholm L, Volin K J, Hitterman R L, Grace J D, Schuller I K, Segre C V, Zhang K and Kleefisch M S 1987 *Phys. Rev.* B **36** 3608
[5] Xiao G, Bakhshai A, Cieplak Z, Tesanovic Z and Chien C L 1988 *Phys. Rev.* B **39** 315
[6] Hasegawa T, Kishio K, Aoki M, Ooba N, Kitawaza K, Fueki K, Uchida S and Tanaka S 1987 *Japan. J. Appl. Phys.* **26** 337
[7] Cieplak M Z, Xiao G, Bakhshai A and Chien C L 1989 *Phys. Rev.* B **39** 4222
[8] Ellman B, Jaeger H M, Katz D P, Rosenbaum T F, Cooper A S and Espinosa G P 1989 *Phys. Rev.* B **39** 9012
[9] Appleman E H, Morss L R, Kini A M, Gieser V, Umezawa A, Crabtree G W and Carlson K D 1987 *Inorg. Chem.* **26** 3237
[10] Nazzal A I, Lee V Y, Engler E M, Jacowitz R D, Tokura Y and Torrance J B 1988 *Physica* C **153** 1367
[11] Tarascon J M, Greene L H, McKinnon W R, Hull G W and Geballe T H 1987 *Science* **235** 1373
[12] Mott N F and Davis E A 1979 *Electronic Processes in Non-Crystalline Materials* 2nd edn (London: Oxford University Press)
[13] Mott N F 1969 *Phil. Mag.* **19** 635
[14] Kwok R S, Cheong S W, Thompson J D, Fisk Z, Smith J L and Wills O J 1988 *Physica* C **152** 240

[15] Tamegai T, Koga K, Suzuki K, Ichihara M, Sakai F and Iye Y 1989 *Japan. J. Appl. Phys.* **28** L112
[16] Yoshizaki R, Saito Y, Abe Y and Ikeda H 1988 *Physica* C **152** 408
[17] Mandal P, Poddar A, Ghosh B and Choudhury P 1991 *Phys. Rev.* B **43** 13 102
[18] Jayaram B, Lanchester P C and Weller M T 1991 *Phys. Rev.* B **43** 5444
[19] Ma M and Lee P A 1985 *Phys. Rev.* B **32** 5668
[20] Ambegaokar V, Halperin B I and Langer J S 1971 *Phys. Rev.* B **4** 2612
[21] Greene R L, Maletta H, Plaskett T S, Bednorz J G and Müller K A 1987 *Solid State Commun.* **63** 379
[22] Ziman J M 1979 *Principles of the Theory of Solids* (Cambridge: Cambridge University Press) p 220
[23] Narlikar A V 1990 *Proc. Int. Conf. on Superconductivity (Bangalore, 1990)* (Singapore: World Scientific) p 103
[24] Jayaram B, Agarwal S K, Narasimha Rao C V and Narlikar A V 1988 *Phys. Rev.* B **38** 2903
[25] Narasimha Rao C V, Jayaram B, Agarwal S K and Narlikar A V 1988 *Physica* C **152** 479
[26] Agarwal S K, Suryanarayanan R, Gorochov O, Moorthy V N and Narlikar A V 1991 *Int. Conf. on Rare Earths Developments and Applications (ICRE '91) (Beijing, 1991)* (Beijing: International Academic Publishers)